

An H I absorption distance to the black hole candidate X-ray binary MAXI J1535–571

Jaiverdhan Chauhan^{1*}, James C.A. Miller-Jones¹, Gemma E. Anderson¹, Wasim Raja², Arash Bahramian¹, Aidan Hotan², Balt Indermuehle², Matthew Whiting², James R. Allison³, Craig Anderson², John Bunton², Baerbel Koribalski², Elizabeth Mahony²

¹International Centre for Radio Astronomy Research – Curtin University, GPO Box U1987, Perth, WA 6845, Australia

²CSIRO Astronomy and Space Science, Australia Telescope National Facility, PO Box 76, Epping NSW 1710, Australia

³Sub-Dept. of Astrophysics, Department of Physics, University of Oxford, Denys Wilkinson Building, Keble Rd., Oxford, OX1 3RH, UK

Accepted XXX. Received YYY; in original form ZZZ

ABSTRACT

With the Australian Square Kilometre Array Pathfinder (ASKAP) we monitored the black hole candidate X-ray binary MAXI J1535–571 over seven epochs from 21 September to 2 October 2017. Using ASKAP observations, we studied the H I absorption spectrum from gas clouds along the line-of-sight and thereby constrained the distance to the source. The maximum negative radial velocities measured from the H I absorption spectra for MAXI J1535–571 and an extragalactic source in the same field of view are $-69 \pm 4 \text{ km s}^{-1}$ and $-89 \pm 4 \text{ km s}^{-1}$, respectively. This rules out the far kinematic distance ($9.2 \pm 0.2 \text{ kpc}$), giving a likely value of $4.0 \pm 0.2 \text{ kpc}$, with a strong upper limit of the tangent point at 6.6 kpc . These distance limits indicate that the peak luminosity of MAXI J1535–571 was > 75 per cent of the Eddington luminosity, and shows that the soft-to-hard spectral state transition occurred at the very low luminosity of $1.2\text{--}3.3 \times 10^{-5}$ times the Eddington luminosity. Finally, this study highlights the capabilities of new wide-field radio telescopes to probe Galactic transient outbursts, by allowing us to observe both a target source and a background comparison source in a single telescope pointing.

Key words: black hole physics – ISM: jets and outflows – radio continuum: stars – X-rays: binaries – X-rays: individual: MAXI J1535–571

1 INTRODUCTION

Stellar-mass black holes in binary systems play an important role in understanding the universal phenomena of accretion and ejection (Fender, Belloni, & Gallo 2004), as they evolve on humanly observable time-scales. However, black hole X-ray binaries (XRBs) typically have poorly constrained distances, with uncertainties often more than 50% (Jonker & Nelemans 2004). The distance of a stellar object is of great importance as it enables us to determine the physical parameters from observables, such as luminosity from flux, physical separation from angular separation, and velocity from proper motion.

Parallax is the most fundamental and model-independent method for estimating stellar distances. The

main caveat of this method is that for typical XRB distances, the measured parallax is extremely small (1 milliarcsec for 1 kpc). Therefore, instruments capable of probing sub-milliarcsecond scales are required. Such studies are possible only with very long baseline interferometry (VLBI) and *Gaia* (Gaia Collaboration et al. 2018), and only for a handful of XRBs (e.g. Miller-Jones et al. 2009; Reid et al. 2011; Gandhi et al. 2019).

High-precision trigonometric parallax measurements are not possible for most black hole XRBs. In such cases, the distance is commonly estimated by comparing the inferred absolute magnitude of the donor star (as determined from its spectral type) with the apparent magnitude, after considering the maximum contribution from the accretion disk (Jonker & Nelemans 2004). The main limitations of this technique are the uncertainties associated with the disk contribution and the extinction along the line of sight.

* E-mail: j.chauhan@student.curtin.edu.au (JC)

If the companion star is too faint (e.g. if the system is highly extinguished) then other methods must be used, one of which uses the Doppler shifted 21-cm absorption line of neutral hydrogen (H I; e.g. Koribalski et al. 1995; Dhawan, Goss, & Rodríguez 2000; Lockman, Blundell, & Goss 2007). Intervening interstellar H I clouds are presumed to follow the rotation of the Milky Way and their absorption features allow us to constrain the kinematic distance to the source (Gathier, Pottasch, & Goss 1986; Kuchar & Bania 1990).

On 2 September 2017, an uncatalogued XRB was co-discovered by the Monitor of All-sky X-ray Image¹ (*MAXI*; Matsuoka et al. 2009) and the Neil Gehrels Swift Observatory (*Swift*; Gehrels, et al. 2004), and designated MAXI J1535–571 (Negoro et al. 2017a; Kennea et al. 2017a). In J2000.0 coordinates, the source is located at RA = 15:35:19.714±0.007, DEC = –57:13:47.583±0.024 (Russell et al. 2017a). Multi-wavelength studies of the system strongly suggest that the accreting compact object is a stellar-mass black hole (Dincer 2017; Kennea 2017b; Negoro et al. 2017b; Russell et al. 2017a,b). However, the physical parameters, including the black hole mass and distance, and the peak luminosity of the outburst are still uncertain.

In this study, we aim to constrain the distance to MAXI J1535–571 using H I absorption spectra from Australian Square Kilometre Array Pathfinder (ASKAP) early science observations. ASKAP is a synthesis radio telescope located at the Murchison Radio-astronomy Observatory (MRO) in Western Australia, which has already established its ability to detect H I absorption from extragalactic sources (Allison et al. 2015, 2017). The telescope operates in the frequency range 0.7–1.8 GHz providing an angular resolution of 10 arcsec and a field of view (FOV) of 30 deg² at 1.4 GHz (Hotan et al. 2014). This allows us to simultaneously measure the H I absorption towards both MAXI J1535–571 and an extragalactic calibrator source, allowing us to distinguish between near and far kinematic distances.

In Sections 2 and 3, we present detailed information on our observations and data reduction techniques, and the obtained H I absorption spectra, respectively. Section 4 discusses the significance of our results. Section 5 contains our conclusions.

2 OBSERVATIONS AND DATA REDUCTION

During the 2017 outburst of MAXI J1535–571, ASKAP observed the source over seven epochs from 21 September to 2 October 2017. At the time of these early science observations, ASKAP was operated in a sub-array of twelve dishes, which provides an angular resolution of ~ 30 arcsec. All observations were conducted at a central frequency of 1.34 GHz with a processed bandwidth of 192 MHz. The total bandwidth was further divided into 10368 fine channels, each with a frequency resolution of 18.519 kHz, with visibilities recorded every 10 s. Further details of the observations can be seen in Table 1.

We reduced our measurement sets using the standard ASKAP data analysis software, *ASKAPsoft*² (pipeline version 0.23.0–beta–10058). For continuum imaging, we per-

formed dynamic flagging of faulty antennas, faulty channels, and baselines affected by radio frequency interference (RFI) during bandpass calibration. Bandpass and flux calibration were performed using the calibrator source PKS B1934–638, and the bandpass solution was interpolated across frequencies where data were flagged. The *IMFIT* task in the Common Astronomy Software Application (CASA v5.1.2-4; McMullin et al. 2007) package was used for measuring the flux densities and 1σ uncertainties of MAXI J1535–571 from the continuum images, which are listed in Table 1.

With a flux density > 150 mJy during the first four epochs, there was enough signal-to-noise to detect H I absorption towards MAXI J1535–571. We used the *SIMAGER* task to generate spectral-line cubes, and performed only stokes-V flagging to avoid removing the true absorption line in the H I region. We applied the bandpass solutions to the raw spectral data and extracted a sub-spectral cube with 1000 channels centered at 1.42 GHz and a velocity resolution of ~ 4 km/s. Note that our conclusions should not be affected by the Galactic H I absorption towards PKS B1934–638, which is very narrow (FWHM < 6 km/s; approximately one channel wide) and therefore only affects the H I absorption line at the rest velocity (0 km/s) (Dénes et al. 2018). We extracted the H I spectra corresponding to MAXI J1535–571 and a nearby extragalactic comparison source PMN J1533–5642 (= MGPS J153358–564218; Griffith & Wright 1993; Murphy et al. 2007), located at RA = 15:33:57.439±39, DEC = –56:42:17.183±39, and analysed the H I absorption complexes with significance exceeding 3σ .

3 RESULTS

The continuum image of the region around MAXI J1535–571 for the 21 September 2017 observation is shown in Figure 1 (left panel), where the source is detected at high significance ($> 200\sigma$). Figure 1 (left panel) also shows the extragalactic comparison source MGPS J153358–564218 with a measured flux density of 340 ± 2 mJy on 21 September 2017, which remained stable to better than 10% between all the epochs.

In the right panel of Figure 1, we present the 1.34 GHz light curve of MAXI J1535–571 from 21 September to 2 October 2017. During this period we observed two distinct peaks on 21 and 23 September, reaching flux densities > 450 mJy, likely corresponding to separate flaring events. Subsequently, the radio flux density of MAXI J1535–571 gradually decreased, reaching a level of ~ 20 mJy by 2 October.

We downloaded the on-demand light curves from *MAXI* in the energy range 2.0–20.0 keV to create a hardness-intensity diagram (HID) for MAXI J1535–571, presented in Figure 2. From the HID, all our radio observations were taken in the soft-intermediate spectral state (Tao et al. 2018). This confirms that MAXI J1535–571 underwent radio flaring behaviour during the hard-to-soft X-ray spectral state transition, as is typical for XRBs (Fender, Belloni, & Gallo 2004).

3.1 H I absorption spectra

In Figure 3, we show the H I spectrum for MAXI J1535–571 for the first epoch (21 September 2017). In the same plot, we also display the spectrum for the extragalactic source MGPS J153358–564218, and the 3σ rms noise levels for the

¹ <http://maxi.riken.jp/top/index.html>

² <http://www.atnf.csiro.au/computing/software/askapsoft/sdp/docs/current/index.html>

Table 1. Details of our ASKAP observations of MAXI J1535–571.

Observation ID	Observation Start date (DD-MM-YYYY)	Observation Start time (hh:mm:ss)	MJD ^a	Exposure time (hh:mm:ss)	Flux Density ^b (mJy)	rms noise (mJy beam ⁻¹)
4340	21-09-2017	03:06:32	58017.17	02:02:26	579.6 ± 2.2	2.0
4364	22-09-2017	01:30:02	58018.12	02:51:50	156.1 ± 2.1	1.8
4367	22-09-2017	10:35:41	58018.50	03:00:56	306.1 ± 1.6	1.2
4374	23-09-2017	13:23:39	58019.58	01:00:52	478.2 ± 2.4	2.2
4410	30-09-2017	03:29:59	58026.23	04:00:56	39.8 ± 0.8	0.5
4414	01-10-2017	03:35:00	58027.23	04:01:01	26.3 ± 0.8	0.5
4418	02-10-2017	03:39:59	58028.24	04:01:22	21.4 ± 0.7	0.5

^a Mid point of our observations,

^b 1σ errors are quoted, calculated by adding in quadrature the 1σ error on the Gaussian fit and the 1σ rms noise in the image.

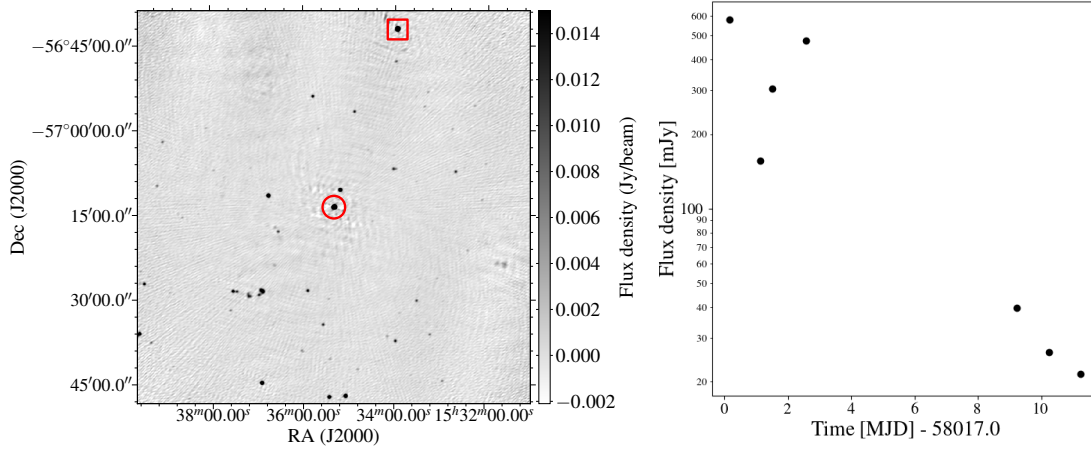


Figure 1. **Left** panel: 1.34 GHz ASKAP continuum image of our 21 September 2017 observation centered at RA = 15:35:19.71, DEC = $-57:13:47.58$ with a size of $1.15^\circ \times 1.15^\circ$. The positions of MAXI J1535–571 and the comparison extragalactic source MGPS J153358–564218 are indicated by the red circle and square, respectively. **Right** panel: ASKAP light curve of MAXI J1535–571 at 1.34 GHz. The peak flux density of MAXI J1535–571 exceeded 500 mJy.

spectra of both sources. In the case of MAXI J1535–571, we observed a significant ($> 3\sigma$) H I absorption complex with a maximum negative velocity of $-69 \pm 4 \text{ km s}^{-1}$. In the second epoch, the H I absorption lines are weaker due to the lower flux density. The third and fourth epochs are excluded from this analysis due to the presence of RFI in the H I spectrum.

For Galactic longitudes $270^\circ \leq l \leq 360^\circ$, the expected radial velocities from Galactic rotation are negative. Figure 4 shows the calculated variation of velocity of the local standard of rest (V_{LSR}) with distance from the Sun (d) in the direction of MAXI J1535–571. For the determination of V_{LSR} , we presumed the Galactic rotation curve to be flat with a circular velocity (V_0) and a Galactic centre distance (R_0) of $236 \pm 3 \text{ km s}^{-1}$ and $8.2 \pm 0.1 \text{ kpc}$ (Bland-Hawthorn & Gerhard 2016; Kawata et al. 2019), respectively. V_{LSR} is symmetric about the tangent point distance ($R = R_0 \cos l$), and therefore provides two estimates of the distance, near and far, within the solar circle. Beyond $d = 13.2 \text{ kpc}$, where $R > R_0$, V_{LSR} becomes positive. Using the maximum negative observed absorption velocity, we constrain the near and far source distances to be $4.0 \pm 0.2 \text{ kpc}$ and $9.2 \pm 0.2 \text{ kpc}$, respectively.

The H I absorption spectrum of the extragalactic source MGPS J153358–564218 (Figure 3) shows $> 3\sigma$ significance absorption out to a maximum negative velocity of $-89 \pm 4 \text{ km s}^{-1}$, which is due to more distant gas clouds,

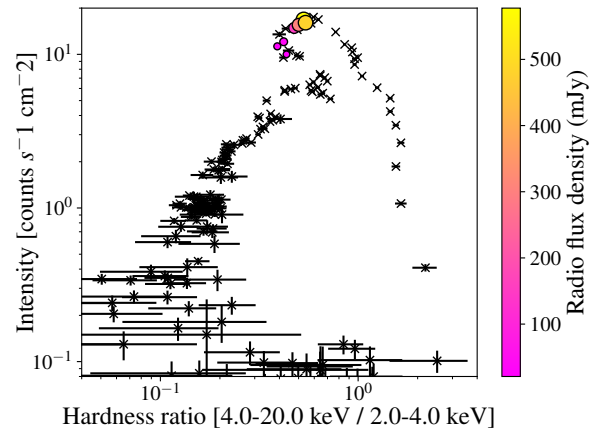


Figure 2. Hardness intensity diagram (HID) for the 2017 outburst of MAXI J1535–571. The HID is made from public MAXI data (Matsuoka et al. 2009), where intensity is the count rate in the energy range 2.0–20.0 keV, and the hardness ratio is the ratio of count rates in the 4.0–20.0 keV and 2.0–4.0 keV energy bands (Tao et al. 2018). Those X-ray data-points with simultaneous radio detections are highlighted with circles, whose size and color correspond to the measured radio flux density. The radio flare occurred during the hard-to-soft X-ray spectral state transition.

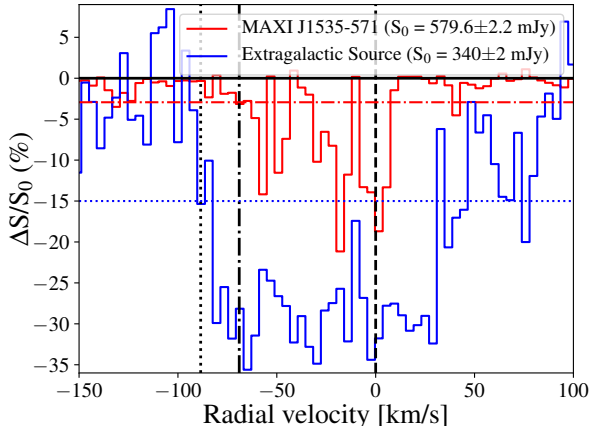


Figure 3. The H I absorption spectrum observed from MAXI J1535–571 on 21 September 2017, when the source was brightest ($S_0 = 579.6 \pm 2.2$ mJy). Spectra of MAXI J1535–571 and the extragalactic source MGPS J153358–564218 (in the local standard of rest frame) are displayed in red and blue, respectively. The solid black horizontal line shows the zero flux level. The red dash-dotted and blue dotted horizontal lines represent the 3σ rms noise levels for MAXI J1535–571 (~ 0.017 Jy beam $^{-1} \equiv 3\%$ of continuum flux density) and the extragalactic source (~ 0.051 Jy beam $^{-1} \equiv 15\%$ of continuum flux density), respectively. The latter is higher due to being located further out in the primary beam. The dashed vertical line shows the rest velocity. The maximum negative velocity of significant ($> 3\sigma$) absorption in the MAXI J1535–571 spectrum (dash-dotted vertical line at -69 km s $^{-1}$) places a lower limit on the source distance of 4.0 ± 0.2 kpc. The maximum negative velocity derived from the extragalactic source spectrum (dotted vertical line at -89 km s $^{-1}$) constrains the upper limit on the distance of MAXI J1535–571 to be that of the tangent point at 6.6 kpc.

and consistent (within uncertainties) with the tangent point velocity of -96 ± 4 km s $^{-1}$. Absorption at the tangent point velocity is not seen towards MAXI J1535–571, implying that MAXI J1535–571 should be located closer than the tangent point distance of 6.6 kpc (Figure 4).

4 DISCUSSION

In the case of MAXI J1535–571, we observed H I absorption lines out to a maximum negative radial velocity of -69 ± 4 km s $^{-1}$ (Figure 3), likely due to the Scutum-Centaurus arm of the Milky Way, which is lying between MAXI J1535–571 and the Sun (Figure 4). This places a lower limit of 4.0 ± 0.2 kpc on the distance to the source. More negative radial velocities (out to -89 ± 4 km s $^{-1}$) are detected towards the extragalactic source and must be coming from larger distances, out to at least the tangent point at 6.6 kpc. If we discount the unlikely scenario that all absorption at intermediate velocities comes from gas clouds more distant than the tangent point, we find a most probable distance of 4.0 ± 0.2 kpc for MAXI J1535–571, placing it close to the inner edge of the Scutum-Centaurus arm. In the following subsections we discuss the implications of these distance constraints.

4.1 Spectral state transition luminosity

According to Kalemci et al. (2013), the soft-to-hard spectral state transition in black hole XRBs usually occurs between

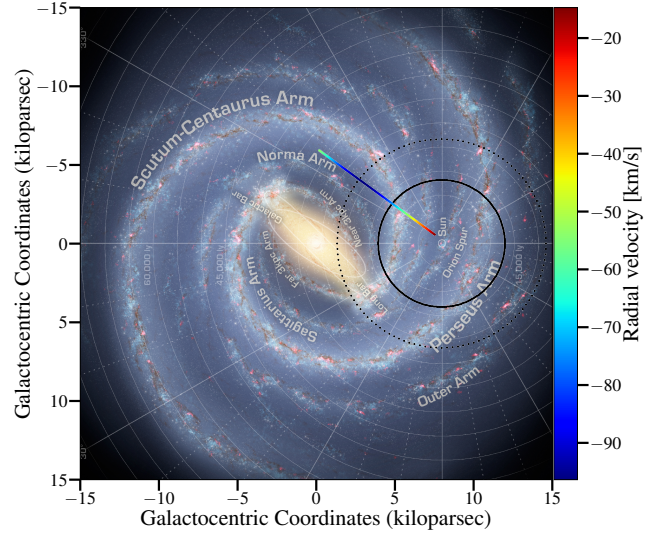


Figure 4. The variation of V_{LSR} with distance from the Sun along the line of sight to MAXI J1535–571, overlaid on a schematic of the Milky Way. The Scutum-Centaurus arm of the Milky Way lies in-between the Sun and MAXI J1535–571. The color bar displays the variation of the predicted velocity (for circular rotation) of the local standard of rest (V_{LSR}) as a function of distance from the Sun (d), in the direction of MAXI J1535–571. The thick and the dashed circles correspond to the most likely distance (4.0 ± 0.2 kpc) and the robust upper limit (6.6 kpc), respectively. We place MAXI J1535–571 beyond the Scutum-Centaurus arm but within 6.6 kpc.

0.3 and 3 per cent of the Eddington luminosity. A *Swift*/XRT observation on 29 April 2018 was identified as the point of the soft-to-hard spectral state transition (Tao et al. 2018), with an unabsorbed X-ray flux of $\sim 6 \times 10^{-12}$ erg cm $^{-2}$ s $^{-1}$. Using our distance estimates, and assuming a typical black hole mass of $8 \pm 1 M_{\odot}$ (Kreidberg et al. 2012), we calculate a transition luminosity of 1.2×10^{-5} times the Eddington luminosity, which is much lower than is typical for black hole XRBs (Kalemci et al. 2013).

Such peculiar behavior has been seen in a few other sources, and a possible explanation was suggested by Vahdat Motlagh, Kalemci, & Maccarone (2019). They hypothesised that an outburst decay could be suspended by a new episode of accretion, which would restart the thermal (soft) emission and send the source into a new soft spectral state. This new soft state would occur at a lower luminosity than normal (0.3 – 3 % of the Eddington luminosity), and therefore the transition to the hard spectral state would take place at a lower Eddington fraction.

4.2 Peak X-ray luminosity

Stiele & Kong (2018) observed a peak X-ray flux of $\sim 3.7 \times 10^{-7}$ erg cm $^{-2}$ s $^{-1}$ (absorbed) from MAXI J1535–571 in the energy range 0.6–10 keV. Using our derived distance constraint of 4.0 ± 0.2 kpc, this corresponds to an absorbed luminosity of 7.1×10^{38} ergs $^{-1}$. For a compact object of typical black hole mass $8 \pm 1 M_{\odot}$ (Kreidberg et al. 2012), this corresponds to ~ 75 per cent of the Eddington luminosity. Tao et al. (2018) reported that over the peak of the outburst, the X-ray spectrum could be fit with a slim disk model,

suggesting a luminosity close to the Eddington luminosity. This is therefore consistent with our distance estimate.

4.3 Line-of-sight hydrogen column density

From our distance constraints and Galactic latitude (b), we infer MAXI J1535–571 to lie 0.08–0.13 kpc below the Galactic plane, well within the scale height of the Milky Way disk (~ 0.3 kpc; Mandel 2016). Using X-ray spectroscopy, the absorption column density (n_{H}) towards MAXI J1535–571 was found to be in the range $2.8 - 5.6 \times 10^{22} \text{ cm}^{-2}$ (Miller et al. 2018; Stiele & Kong 2018; Tao et al. 2018), which is consistent with the predicted Galactic absorption value of $2.0 \pm 1.0 \times 10^{22} \text{ cm}^{-2}$ in the direction of MAXI J1535–571, calculated from the extinction maps and estimated correlation between n_{H} and A_{V} (Schlafly & Finkbeiner 2011; Bahramian et al. 2015; Foight, Güver, Özel & Slane 2016). The high value of n_{H} for MAXI J1535–571 is probably due to enhanced absorption in the Scutum-Centaurus arm of the Milky Way, through which we view MAXI J1535–571.

5 SUMMARY

In this study, we measured a kinematic distance to the black hole candidate XRB MAXI J1535–571 using an H I absorption spectrum obtained from ASKAP early science observations. A comparison extragalactic source in the same field shows H I absorption out to $-89 \pm 4 \text{ km s}^{-1}$ (consistent with coming from the tangent point at 6.6 kpc), whereas MAXI J1535–571 shows no H I absorption beyond $-69 \pm 4 \text{ km s}^{-1}$. Therefore, the most probable distance to the source is 4.0 ± 0.2 kpc, with a robust upper limit of 6.6 kpc.

Our distance constraints have confirmed that MAXI J1535–571 was accreting close to the Eddington rate at the peak of the outburst, in agreement with X-ray spectral fitting results by Tao et al. (2018). We also demonstrate that the soft-to-hard X-ray spectral state transition in MAXI J1535–571 occurred at a very low fraction ($1.2 - 3.3 \times 10^{-5}$) of the Eddington luminosity, which could be due to a second episode of accretion partway through the outburst decay.

This study also highlights the importance of modern radio telescopes such as ASKAP, which provide both high sensitivity and a wide field of view. In this project, the wide field of view of ASKAP afforded us the opportunity to study the H I absorption spectrum of both MAXI J1535–571 and a comparison extragalactic source within the same observation. The high sensitivity and high spectral resolution of ASKAP allowed us to extract the H I spectrum from just two hours of observation, placing stringent constraints on the distance to MAXI J1535–571.

ACKNOWLEDGEMENTS

The Australian SKA Pathfinder is part of the Australia Telescope National Facility which is managed by CSIRO. Operation of ASKAP is funded by the Australian Government with support from the National Collaborative Research Infrastructure Strategy. ASKAP uses the resources of the Pawsey Supercomputing Centre. Establishment of ASKAP, the Murchison Radio-astronomy Observatory and the Pawsey Supercomputing Centre are initiatives of the Australian Government, with support from the Government of Western Australia and the Science and Industry Endowment Fund. We acknowledge the Wajarri Yamatji people

as the traditional owners of the Observatory site. JCAM-J is the recipient of Australian Research Council Future Fellowship (project number FT140101082) and GEA is the recipient of an Australian Research Council Discovery Early Career Researcher Award (project number DE180100346) funded by the Australian Government.

REFERENCES

- Allison J. R., et al., 2015, *MNRAS*, 453, 1249.
 Allison J. R., et al., 2017, *MNRAS*, 465, 4450.
 Bahramian A., Heinke C. O., Degenaar N., Chomiuk L., Wijnands R., Strader J., et al., 2015, *MNRAS*, 452, 3475.
 Bland-Hawthorn J., Gerhard O., 2016, *ARA&A*, 54, 529.
 Dénes H., McClure-Griffiths N. M., Dickey J. M., Dawson J. R., Murray C. E., 2018, *MNRAS*, 479, 1465.
 Dhawan V., Goss W. M., Rodríguez L. F., 2000, *ApJ*, 540, 863.
 Dincer T., 2017, *ATel*, 10716.
 Fender R. P., Belloni T. M., Gallo E., 2004, *MNRAS*, 355, 1105.
 Foight D. R., Güver T., Özel F., Slane P. O., 2016, *ApJ*, 826, 66.
 Gaia Collaboration, et al., 2018, *A&A*, 616, A1.
 Gandhi P., Rao A., Johnson M. A. C., Paice J. A., Maccarone T. J., 2019, *MNRAS*, 485, 2642.
 Gathier R., Pottasch S. R., Goss W. M., 1986, *A&A*, 157, 191.
 Gehrels N., et al., 2004, *ApJ*, 611, 1005.
 Griffith M. R., Wright A. E., 1993, *AJ*, 105, 1666.
 Hotan A. W., et al., 2014, *PASA*, 31, e041.
 Jonker P. G., Nelemans G., 2004, *MNRAS*, 354, 355.
 Kalemci E., Dincer T., Tomsick J. A., Buxton M. M., Bailyn C. D., Chun Y. Y., 2013, *ApJ*, 779, 95.
 Kawata D., Bovy J., Matsunaga N., Baba J., 2019, *MNRAS*, 482, 40.
 Kennea J. A., Evans P. A., Beardmore A. P., Krimm H. A., Romano P., et al., 2017a, *ATel*, 10700.
 Kennea J. A., 2017b, *ATel*, 10731.
 Koribalski B., Johnston S., Weisberg J. M., Wilson W., 1995, *ApJ*, 441, 756.
 Kreidberg L., Bailyn C. D., Farr W. M., Kalogera V., 2012, *ApJ*, 757, 36.
 Kuchar T. A., Bania T. M., 1990, *ApJ*, 352, 192.
 Lockman F. J., Blundell K. M., Goss W. M., 2007, *MNRAS*, 381, 881.
 Mandel I., 2016, *MNRAS*, 456, 578.
 Matsuoka M., et al., 2009, *PASJ*, 61, 999.
 McMullin J. P., Waters B., Schiebel D., Young W., Golap K., 2007, *ASPC*, 376, 127.
 Miller J. M., et al., 2018, *ApJ*, 860, L28.
 Miller-Jones J. C. A., Jonker P. G., Dhawan V., Brisken W., Rupen M. P., Nelemans G., Gallo E., 2009, *ApJ*, 706, L230.
 Murphy T., Mauch T., Green A., Hunstead R. W., Piestrzynska B., Kels A. P., Sztajer P., 2007, *MNRAS*, 382, 382.
 Negoro H., et al., 2017a, *ATel*, 10699.
 Negoro H., et al., 2017b, *ATel*, 10708.
 Reid M. J., McClintock J. E., Narayan R., Gou L., Remillard R. A., Orosz J. A., 2011, *ApJ*, 742, 83.
 Russell T. D., Miller-Jones J. C. A., Sivakoff G. R., Tetarenko A. J., Jacpot Xrb Collaboration, 2017a, *ATel*, 10711.
 Russell T. D., Altamirano D., Tetarenko A. J., Sivakoff G. R., et al., Jacpot Xrb Collaboration, 2017b, *ATel*, 10899.
 Schlafly E. F., Finkbeiner D. P., 2011, *ApJ*, 737, 103.
 Stiele H., Kong A. K. H., 2018, *ApJ*, 868, 71.
 Tao L., et al., 2018, *MNRAS*, 480, 4443.
 Vahdat Motlagh A., Kalemci E., Maccarone T. J., 2019, *MNRAS*, 485, 2744.

This paper has been typeset from a $\text{\TeX}/\text{\LaTeX}$ file prepared by the author.